

Diesel-Biodiesel Blends Production, applied in the BD 5.0 Internal Combustion Engine to Evaluate the Future of Brazil's Biodiesel Energy Matrix

José D. Pinilla ^{a,d*}, Manuel A. Mayorga ^{b,d}, Henrique H. Junqueira ^c, Alexandre S. Dos Santos ^a, Rogerio A. Melo ^a, Marcela C. Nery ^a

^a Universidade Federal dos Vales de Jequitinhonha e Mucuri, Programa de Pós-graduação em Biocombustíveis, Diamantina MG, Brazil.

^b Universidad Libre, Avenida 70 # 53-40, Bogotá D.C, Colombia.

^c Usina de biodiesel Petrobrás, Avenida das indústrias 531 Distrito industrial, Montes Claros MG, Brazil MG, Brasil.

^d Universidad ECCI, Grupo de Investigación GIATME, Bogotá D.C, Colombia.

pinilla.david@ufvjm.edu.br

In South America, Brazil is the largest producer of biofuels in the world. This country has the fifth position with a significant opportunity to produce more biofuels, with potential in the biodiesel sector. Currently, in the country's transportation sector, the proportion of distribution of biodiesel blends with petrol diesel is 14%- B14, and the following year, it will be 15%- B15 until it reaches 20% or B20 in 2030. All this is to accomplish the United Nations' sustainable development goals in their numerals: 7 about clean energy, 9 about industry, innovation, and infrastructure, 11 about sustainable cities, 12 about responsible consumption and production, and the last 13 about climate action. The principal objective of this study is to evaluate the BD 5.0 diesel engine's behavior with different blends, obtain different parameters, and generate simulation in emissions results using the software DIESEL RK, all this to have a better technological alternative prediction route to apply in future blends of biodiesels. The results show significant correlations between the heat value in the biodiesel blends and the engine fuel consumption. In the developed simulations, lean fuel mixtures λ of 1,5 are applied in the internal combustion engine, decreasing the temperature in the engine combustion chamber at high biodiesel blends, increasing the CO₂ levels, and diminishing the NO_x emissions, whereas at low biodiesel blends cold alternatives of combustion can diminish the temperature in the combustion engines chambers.

1. Introduction

In the world, Brazil is the 2nd country in biodiesel production, with approximately 8 million of m³ in 2024 (ANP., 2024); the country has a significant opportunity to expand its oilseeds crop matrix by a wide variety of sources apart from the traditional soybean (*Glycine max*), animal fats, used cooking oil, cotton seeds (*Gossypium herbaceum*), canola oil (*Brassica campestris*), and corn oil (*Zea mays*), by other interesting non-edible oils resources like macauba (*Acrocomia aculeata*), dende (*Elaeis guineensis*), inajá (*Attalea maripa*), tucumã (*Astrocaryum aculeatum* G.), pinhão manso (*Jatropha curcas*), and mamona (*Ricinus communis*), (Hayder A., Alalwan., 2019). The diversification of raw materials diminishes dependence on only one oleaginous resource crop, which can be unstable due to climatic changes and the probable proliferation of dangerous plagues. A higher percentage of biodiesel blends utilized in internal combustion engines can develop better lubricity by their chemical double bond components, such as methyl linoleate C₁₉H₃₂O₂ and methyl oleate C₁₉H₃₆O₂, with more equilibrium in CO₂ emissions produced than can be reabsorbed by the plants to close their natural cycle, resulting in a more clean mobility.

2. Methodology

With the physiochemical characterization of biodiesel B100, provided by the PETROBRAS biodiesel plant in Montes Claros MG, Brazil to accomplish the ABNT requirements; were elaborated different blends, starting from the commercial biodiesel- diesel B14, growing the quantity of biodiesel to obtain samples of 600 ml of B20, B25, B30, B40, B50, B70, B80, and B100, these blends was characterized in chromatographic gas analyzer-MS Shimadzu, Model GCMS-QP2010, which belongs to the multipurpose laboratory of University UFU in Itaiuticaba, MG, Brazil and evaluated in the UFVJM, campus II Diamantina MG in their density (specific mass), kinematic viscosity made by viscometer Brookfield Digital DV-III and the heat value made by a calorimeter bomb IKA C5010 5012, all these characterization results were included in the simulation software Diesel RK where were introduced parameters like fuel characterization, engine configuration, fuel injection system, combustion chamber, gas exchange, and turbocharging system to be part to obtain approximate results to compare with the realized engine tests. Figure 1 shows the chromatographic analysis results in the fuel blends with $R > 0,94$. The percentage of biodiesel shown in the abscissa axis significantly increases the components of C18:2 Methyl linoleate and C18:1 methyl oleate, where their double bonds form a dense adsorption film of molecules on the metal surface of the moving parts in the ICE. In minor proportions, components C16:0 and C18:0 represent the methyl palmitate and methyl stearate that increase with more biodiesel added to the blend (Wang., 2021).

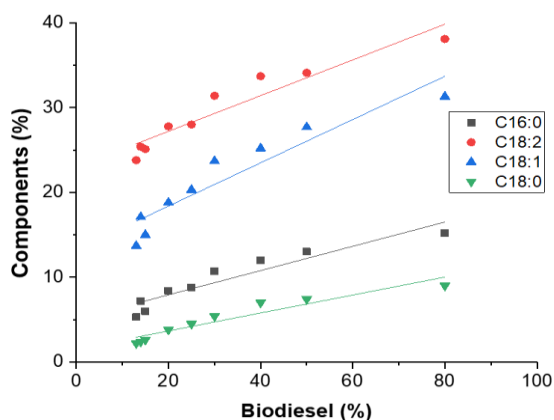


Figure 1. Percentual relations between biodiesel blends and fatty acid methyl esters FAME.

The diesel ICE model BD-5.0 utilized for the tests is a 4-stroke single-cylinder engine with an air-refrigerated block, overhead valve distribution OHV, a direct injection system of $\pm 21^\circ$ CAD BTDC before the top dead center of the piston, and a fuel bomb pressure of 19,6 MPa. The engine specifications are shown in Table 1.

Table 1: Specifications ICE BD 5.0.

Single cylinder Diesel engine BD 5.0 G2		Units
Displaced volume	211	cm ³
Stroke	55	mm
Bore x Stroke	70	mm
Injection system	Direct	-
Compression ratio	20:1	-
Number of Valves	1 for admission and 1 for exhaust	Unit
Refrigeration system	Air	-
Maximum Power	5,0 HP at 3600 rev min ⁻¹	-
Continuous power	4,2 HP at 3600 rev min ⁻¹	-

The dynamometric bench brake system consists of a 7.4 kW electrical engine connected to a load cell of 0,03% F.S. regulated by a potentiometer with variable charge levels from 0 to 100%. The ICE control acceleration is manual. A National Instruments electronic control module ECM NI USB-6009 makes the data acquisition; the configuration of the experimental engine connected to a dynamometric bench is shown in Figure 2.

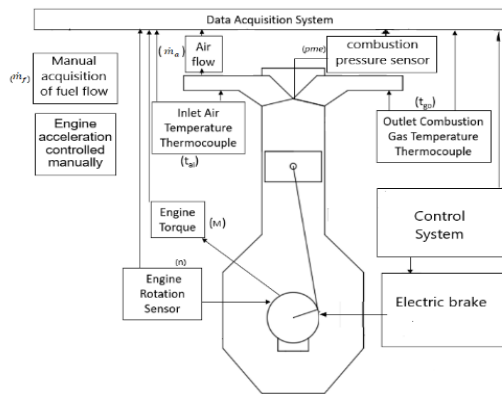


Figure 2: Engine test setup. Adapted from (Claudio Marcio Santana, 2024).

In the Mathematic applications, the Eq(1) of effective medium pressure, emp , is calculated, where N_e is the effective power, V_T is the volume of displacement of the engine, n are the revolutions of the engine and i is the number of cycles per revolution (González., 2011), this to compare the results between the pressure sensor GEFRAN K30 with precision $< \pm 0,25\%$ FSO (H); $< \pm 0,5 \%$ FSO (M) and the calculated values, where the encountered absolute errors and relatives are $0,08 \text{ kg cm}^{-2}$ and $2,0\%$.

$$emp = \frac{N_e}{V_T n i} \quad (1)$$

The mass flow is calculated in a volumetric way Eq(2), where V is the volume in liters on the test calibration tube, and ρ is the fuel density (specific mass) in g cm^{-3} , and t is the time that it takes for the test tube to be empty in hours depending the level of charge, where the applied specific consumption equation is the Eq(3):

$$\dot{m}_f = \frac{V \rho_c}{t} \quad (2)$$

$$c_e = \frac{\frac{V \rho_c}{t}}{N_e} = \frac{\dot{m}_f}{N_e} \quad (3)$$

Table 2 shows: the Heat Value, H_c ; Cetane number; Density (specific mass) ρ_c ; and Viscosity. These properties were obtained in every diesel-biodiesel blend to be applied in the equations. The calculation of cetane number is obtained from Baharak, Sajjadi (2016).

Table 2: Physiochemical characteristics in biodiesel blends obtaining calorific power, density by NBR 14095, and the kinematic viscosity by NBR 10441 regulations.

Biodiesel blend	Heat value (kJ/kg)	Cetane number	Density at 20 °C (kg m ⁻³)	Viscosity at 40 °C (cP)
B14	45,977	43	852	3,72
B20	45,515	44	854	3,84
B25	45,355	44	855	3,84
B30	45,085	44	856	3,72
B40	44,947	47	858	4,32
B50	43,706	47	861	4,32
B70	43,144	49	864	4,44
B80	42,153	50	870	4,32
B100	42,025	50	875	4,32

2.1 Experimental

All the blends were characterized, and every diesel–biodiesel sample was tested on the dynamometer bench at ambient conditions of temperatures between 23- 28 °C and barometric pressure of 0.89 bar, data are obtained every second regarding maximum torque generated at 2500 (± 50) rev min^{-1} and power at 3600 (± 50) rev min^{-1} , specified by the ICE technical sheet BD 5.0. The potentiometer charges were manually increased to generate more brake power in the ICE.

2.2 Numerical simulation approach

In the software Diesel RK, 2010, based on the thermodynamics first law are introduced the measured engine configuration, ambient conditions of 27 °C and atmospheric pressure of 0,89 and 1,01 bar, fuel characterization, geometrical properties in the cylinder head, heat transfer, and frictional coefficients, design of the combustion chamber coefficient, effective area of piston rings, the relative duration of the injection, ignition time and pressure, diesel injector design, air-fuel equivalence, length of admission and exhaust manifold, dimensions of admission and exhaust valves, to obtain engine performances and emissions characteristics in the proposed fuel blends in constant revolutions and compression ratio (Rajak,U., 2018), with lambda coefficient of 1.5, its given by the sum of available oxygen on the oxygen demanded (Guzella., 2009), as shown in the Eq(4):

$$\lambda = \frac{\Sigma O_{available}}{\Sigma O_{demanded}} \quad (4)$$

3. Results and Discussion

The experiments were conducted to obtain the maximum power and torque for the diesel-biodiesel blends shown in Table 3, with the values of emp, time, and fuel consumption at angular velocities of 3500 and 2500 rev min⁻¹. An ANOVA analysis of power performance is presented in Table 4; the angular velocity (rev min⁻¹) has a statistically significant effect on power. Here, the null hypothesis is rejected because the high F-value and P-value indicate a strong effect; the rev-min⁻¹, with 1 degree of freedom, shows insignificant variation in the developed power (Al-lwayzy., 2017). The biodiesel blend significantly not affect the power development; the null hypothesis is not rejected with 9 degrees of freedom, because the P-value is greater than 0,05; In the interaction between angular velocity and blend is not significant; In the physical effect, the lower heating value of high-percentage in biodiesel blends means that the engine requires more fuel consumption to achieve the power and torque threshold (Wahlen., 2013). In the torque performance shown in Table 5, the angular velocity (Rev-min⁻¹) has a highly significant effect on torque. The null hypothesis is rejected with 1 degree of freedom supported by the results in P-value of 0,00029 and the F-value of 21,23, which is much greater than the F critical of 4,49; In the biodiesel blend factor, don't have significant effect in the torque, the null hypothesis is not rejected; the F-value of 0,549 is less than the F critical of 2,53. The model's variance explained (R²) is 69%. The rev-min⁻¹ contributes with 40.10% of the variance, being the only significant analysis value. The emp tends to decrease with a higher biodiesel content in the diesel-biodiesel blend, due to the lower heat value of high-biodiesel blends. Simulations using Diesel RK software were performed to compare engine performance at two distinct atmospheric pressure conditions: 0.906 bar, corresponding to the high-altitude location of Diamantina, Brazil, at 1384 meters above sea level and 1.01 bar, corresponding to the standard sea-level pressure. All simulation results were established at an angular velocity of 3500 rev min⁻¹.

Table 3. Test results of maximum power, torque, consumption, and emp with different fuel mixtures of biodiesel-diesel.

		Power, kW								
Blend		B14	B20	B25	B30	B40	B50	B70	B80	B100
Angular velocity	2500	4,6	3,9	4,5	4,1	4,1	3,9	3,8	4,6	2,7
	3500	4,2	3,4	3,4	3,4	3,8	3,9	4,0	3,4	4,2
rev min ⁻¹	2500	4,3	4,7	4,5	4,8	4,5	4,9	5,0	4,8	4,6
	3500	4,3	4,2	4,4	4,2	4,5	4,9	5,0	4,6	4,6
		Torque, Nm								
Angular velocity	2500	17,2	15,4	17,4	15,7	15,9	15,3	15,5	17,1	10,7
	3500	17,1	13,4	13,0	13,3	14,4	15,0	15,6	13,4	13,8
rev min ⁻¹	2500	12,1	12,8	12,6	13,4	12,9	13,5	13,9	13,4	12,7
	3500	11,9	11,8	12,5	9,7	12,4	13,5	13,9	12,6	12,7
		Consumption C _e , g/kWh								
Angular velocity	2500	154,3	177,5	166,3	168,3	179,2	182,5	185,4	320,9	447,6
	3500	155,0	190,5	172,0	196,5	198,9	189,5	188,1	379,2	418,6
rev min ⁻¹	2500	200,6	197,7	242,1	219,2	220,4	232,0	363,2	423,5	508,4
	3500	228,7	176,2	243,2	182,9	211,0	239,3	359,5	444,8	507,1
		emp kgf cm ⁻²								
Angular velocity	2500	10,2	9,1	10,3	9,3	9,4	9,0	9,1	8,1	7,2
	3500	10,1	7,9	7,7	7,9	8,5	8,9	9,3	7,9	8,5
rev min ⁻¹	2500	7,2	7,6	7,5	7,9	7,3	8,0	8,2	7,9	7,6
	3500	7,1	7,0	7,4	5,7	7,3	8,1	8,4	7,5	7,6

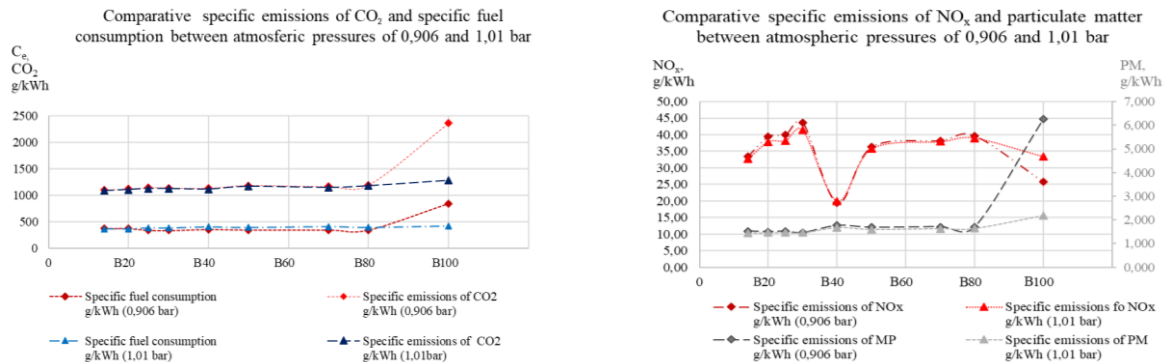
Table 4: ANOVA of engine power performance, angular velocity, and the fuel blend.

Source	Degrees of freedom	SC	CM	F	F Critical	p-value	Reject hypothesis	Significant effect	% of Contribution
Rev min ⁻¹	1	4,43	4,43	21,67	4,49	0,00026	Yes	Yes	45,98
Blend	9	0,82	0,09	0,44	2,53	0,888	No	No	8,55
Interaction	9	1,11	0,123	0,60	2,53	0,776	No	No	11,52
Error	16	3,27	0,204						
Total	35	9,63						R ² =0.66	*R ² =0,45

Table 5: ANOVA of engine torque performance, angular velocity, and the fuel blend.

Source	Degrees of freedom	SC	CM	F	F Critical	p-value	Reject hypothesis	Significant effect	% of Contribution
Rev min ⁻¹	1	46,74	46,74	21,23	4,49	0,00029	Yes	Yes	40,10
Blend	9	17,76	1,97	0,89	2,53	0,549	No	No	15,24
Interaction	9	16,84	1,87	0,85	2,53	0,583	No	No	14,45
Error	18	35,21	2,20						
Total	35	116,56						R ² =0,69	*R ² =0,40

The Specific fuel consumption, C_e , and specific CO₂ emissions, as shown in Figure 3a, exhibited similar trends across both atmospheric pressures for most blends. A divergence occurs after the B80 blend at a pressure of 0,906 bar, where the C_e increases substantially from 346 g kWh⁻¹ at B80 to 837 g kWh⁻¹ at B100; meanwhile, the specific CO₂ emissions increase significantly, rising from 1195 g kWh⁻¹ at B80 to 2539 g kWh⁻¹ at B100. Figure 3b shows the specific NOx emissions, which decrease with increasing blend concentration. At a pressure of 0,906 bar, the specific NOx dropped from 39,63 g kWh⁻¹ at B80 to 25,80 g kWh⁻¹ at B100. At standard pressure of 1,01 bar, the NOx decreased from 38,98 g kWh⁻¹ in B80 to 33.41 g kWh⁻¹ at B100. This reduction is attributed to low combustion-chamber temperature, resulting from the increased fuel required to maintain the target power. A separate test showed NOx emissions decreasing to 19 g kWh⁻¹ at the B40 blend when the intake air temperature was modified to 0°C. In the exhaust particulate matter emissions (PM) demonstrated significant increase after the B80 blend, with the effect being far more pronounced at high altitude: at low pressure of 0,906 bar, the PM increased sharply from 1,698 g kWh⁻¹ to 6,261 g kWh⁻¹; at standard pressure of 1,01 bar the PM increased, but less severely from 1,642 g kWh⁻¹ at B80 to 2,170 g kWh⁻¹ at B100.

Figure 3: Simulation results in software Diesel RK for different biodiesel blends. 3a: Specific fuel consumption C_e and specific emissions of CO₂, 3b: Specific NOx emissions, and specific emissions of particulate matter.

4. Conclusions

The results of the experimental design analysis show that, with a 5% confidence level, the angular frequency (or velocity) is the only factor with a statistically significant effect on both engine power and torque. The statistical models demonstrated good explanatory power, accounting for 66% of the variance in power and 69% in torque. At a 95% confidence level, neither angular velocity nor the fuel blend factor showed a significant effect on specific consumption, C_e , or emp .

The experiments were conducted in the city of Diamantina, Minas Gerais, at 1384 meters above sea level, demonstrating that low oxygen availability significantly increased fuel consumption, particularly after the B80

blend, leading to higher uncontrolled emissions of CO, CO₂, and particulate matter, especially with higher blends. B100 biodiesel has high lubricant properties but a lower heat value than commercial blends like B14. The need to control NO_x emissions remains, and lowering the admitted air temperature is proposed as a viable strategy to mitigate their formation.

Brazil has significant potential to expand oilseed cultivation from non-edible sources across states such as Mato Grosso, Minas Gerais, and São Paulo. This expansion can increase the feasible biodiesel blending ratios and support the nation's efforts to meet the United Nations Sustainable Development Goals for 2030. While it is impossible to eliminate CO₂ from ICE, controlling the emission of these gases through the use of biofuels or e-fuels is essential to reduce the global warming potential and carbon footprint in the transport sector.

Nomenclature

ABNT – Brazilian Association of Technical Standards	N _e – Effective Power
CAD – Crank Angle Degrees	V – Volume, L
CO – Carbon Monoxide	V _T – Volume of Displacement of the Engine
CO ₂ – Carbon Dioxide	n – Revolutions of the Engine
emp – Effective Medium Pressure	i – Number of Cycles per Revolution
FAME – Fatty Acid Methyl Esters	\dot{m}_f – Mass Flow, g h ⁻¹
FS – Full Scale Mass Flow	c _e – Specific Consumption
FSO – Full Scale Output	ρ _c – Density (Specific Mass), g cm ⁻³
ICE – Internal Combustion Engine	t – time in s or h
m ³ – Cubic Meters	λ – Lambda sum of available oxygen on the oxygen demanded
NO _x – Nitrogen Oxides	

Acknowledgments

Universidade Federal dos Vales do Jequitinhonha e Mucuri (UFVJM), Instituto de Ciência y Tecnologia (ICT), e órgãos de fomento CNPq, FAPEMIG e CAPES. Planta PETROBRAS Biocombustível Montes Claros MG Br.

References

- Al-lwayzy, Y. T. (2017). Diesel engine performance and exhaust gas emissions using microalgae *Chlorella protothecoides* biodiesel. *Renewable energy an international journal*, págs. 690-701 <https://doi.org/10.1016/j.renene.2016.09.035>.
- Baharak Sajjadi, A. A. (2016). A comprehensive review on properties of edible and non-edible vegetable oil-based biodiesel: Composition, specifications and prediction models. *Renewable and Sustainable Energy Reviews*, 62-92 <https://doi.org/10.1016/j.rser.2016.05.035>.
- Claudio Marcio Santana, L. L. (01 de 04 de 2024). Experimental analysis of the thermal energy balance of an Otto cycle engine operated with ethanol and gasoline. *SIMEA*, págs. 1-8.
- González, F. P. (2011). *Motores de combustión interna alternativos*. Valencia: Reverté.
- Guzella, L. O. (2009). Introduction to modeling and control of internal combustion engine systems. En G. Lino, *Introduction to modeling and control of internal combustion engine systems* (págs. DOI 10.1007/978-3-642-10775-7). Milan: Springer Science & Business Media.
- Hayder A. Alalwan, A. H. (2019). Promising evolution of biofuel generations. *Subject review, Focus*, 127-139.
- P. McCarthy, M. R. (2011). Analysis and comparison of performance and emissions of an internal combustion engine fueled with petroleum diesel and different bio-diesels. *FUEL*, 2147-2157 <https://doi.org/10.1016/j.fuel.2011.02.010>.
- R.E. Pauls. (2011). A Review of Chromatographic Characterization Techniques for Biodiesel and Biodiesel Blends. *Journal of Chromatographic Science*, 384-396.
- RK, D. (2025 de 02 de 2010). Engine simulation tool DIESEL RK. Obtenido de <https://diesel-rk.com/Eng/>
- UN. (11 de 12 de 2024). <https://sdgs.un.org/goals>. Obtenido de <https://unstats.un.org/sdgs/files/report/2024/SG-SDG-Progress-Report-2024-advanced-unedited-version.pdf>: <https://sdgs.un.org/goals>
- Upendra Rajak, P. N. (2018). Numerical investigation of performance, combustion and emission characteristics of various biofuels. *Energy Conversion and Management*, 235-252 <https://doi.org/10.1016/j.enconman.2017.11.017>.
- Wahlen, B. D. (17 de 01 de 2013). Biodiesel from microalgae, yeast, and Bacteria: Engine Performance and Exhaust Emissions. *American Chemical Society*, pag. 220-228.
- Wang, W. (2021). Effects of unsaturated fatty acid methyl esters on the oxidation stability of biodiesel determined by a gas chromatography-mass spectrometry and information entropy methods. *Renewable energy an internal journal*, 880-886 <https://doi.org/10.1016/j.renene.2021.04.132>